The final publication is available at

https://doi.org/10.1016/j.applthermaleng.2021.117034

Additional Information

Implementation of 1D-3D integrated model for thermal prediction in internal combustion engines

X. Margot, J. Gomez-Soriano, P. Quintero, J. Escalona*

CMT – Motores Térmicos, Universitat Politècnica de València, Camino de Vera, 46022 Valencia, Spain

Abstract

The need to improve the thermal efficiency of gasoline engines used in hybrid vehicles, has led to explore new solutions for reducing engine heat losses. Hence, it is important for the car manufacturers to be able to predict the heat transfer in the engine components. Numerical methods such as CFD (Computational Fluid Dynamics) or CHT (Conjugate Heat Transfer) can be used to assess the heat losses through the combustion chamber walls, but they are long and costly. In this regard, it is particularly interesting for the industry to use simplified models, which may play a key role in the design stage. In this work a 1D model integrated with 3D finite elements based on a commercial software is used to calculate the heat losses in a single-cylinder gasoline direct injection engine. The model is first validated, then a detailed heat transfer analysis is performed, and its results compared to those of a full CFD-CHT simulation. Results demonstrate that this approach is suitable to predict in a short time the heat losses and the spatial temperature distribution in the solid regions of an internal combustion engine. The model also yields accurate values in terms of engine performance.

Keywords: CHT, Combustion, ICE, FEA, Spark engines, Heat transfer model

1. Introduction

In the coming years the automotive industry will direct its efforts to the electrification of the powertrains, among others by developing hybrid vehicles. Therefore, internal combustion engines will remain in use for yet several years. In particular, since the Euro 6 standards have been defined [1], spark ignition engines are bound to dominate the market in detriment of the Diesel engines. Environmental regulations are stricter about cars pollutant emissions and push the manufacturers to design more eco-friendly and efficient engines. New alternatives such as downsizing engines [2, 3], increasing air-fuel ratio, enhancing fuel mixture by using additives [4–6] or coating the combustion chamber walls have been the focus of recent research [7–11]. One of the main targets nowadays is to reduce the heat transfer losses in ICEs and increase their thermal efficiency [12]. Hence, it is important to quantify these losses in order to optimize the design of the engines.

Over the past years, some authors have made important contributions in 1D and 3D modeling for the thermal management in ICEs. For instance, Torregrosa et al. [13] have developed a 1D lumped model to study the heat transfer through the solid walls of an ICE. Nowadays, similar approaches are employed for modelling the heat losses in ICEs [14–20]. In these models, the solid regions are discretized with a finite number of nodes considering certain assumptions to simplify the system. Their advantage in terms of calculation time has been confirmed by several authors [21]. However, the simplified assumptions are their main drawback since they neglect the spatial information.

More recently, advances in CAE (Computer-aided engineering) have allowed the development of 3D calculation tools to study in detail the physical processes that take place in an ICE. Therefore, many works have been carried out to calculate the heat transfer in an ICE by using 3D CFD, CHT and Finite Element Analysis (FEA). Some researchers [22–25] have employed 3D-CFD simulations where isothermal walls are considered for the engine boundaries to study the combustion process. Decoupled models that solve separately the fluid with CFD and the solid domain with FEA are another means to calculate the heat transfer [26]. More efficiently, coupled CFD-CHT methods allow predicting the heat transfer through the combustion chamber walls [27–31]. In general, all these techniques demand important computational resources compared with the 1D models.

New alternative strategies to couple 1D and 3D modeling have been proposed by different authors to obtain a more accurate prediction of heat transfer in ICEs at less computational cost than full 3D methods. In this regard, Bolehovsky et al.[32] developed a fully integrated model of the ICE, which included all the systems, e.g. the

---

*Corresponding author. Tel.: +34 963 877 650,
Email address: xmargot@mot.upv.es (X. Margot), jogoso1@mot.upv.es (J. Gomez-Soriano), pedquiig@mot.upv.es (P. Quintero), joescor2@mot.upv.es (J. Escalona)

Nomenclature

	Abbreviations		IVC	Intake Valve Closing
1D	One dimensional		SI	Spark Ignition
3D	Three dimensional		TDC	Top Dead Center
BDC	Bottom Dead Center			
CAD	Computer-Aided Design			*List of symbols*
CAE	Computer-Aided Engineering		Cp	Calorific power of the fuel $[J/kg]$
CCV	Cyclic-to-cyclic variations		m_{air}	Mass of trapped air at IVC $[kg]$
CFD	Computational Fluid Dynamics		m_{CO}	Mass of CO $[kg]$
CHT	Conjugate Heat Transfer		m_{HC}	Mass unburned HC emissions $[kg]$
CJ	Cooling jacket		m_{fuel}	Injected fuel mass $[kg]$
FE	Finite Element		V_T	Maximum volume of the cylinder $[m^3]$
FEA	Finite Element Analysis		W	Indicated work $[J]$
FIM	Fully Integrated model		ρ	Air density upstream $[kg/m^3]$
HTC	Heat Transfer Coefficient		η_{comb}	Combustion efficiency $[\%]$
ICE	Internal Combustion Engine		η_{ind}	Indicated efficiency $[\%]$
IFPEN	IFP Energy Nouvelles		η_{vol}	Indicated efficiency $[\%]$

after-treatment system, the crank-train mechanism and the hydraulic systems . The same approach was employed by Graziano et al. [33] for the heat rejection prediction in a Diesel engine.

From the methods mentioned above, the CFD-CHT approach seems to be one of the most suitable to study in detail the heat transfer in ICEs [34, 35]. However, it is extremely important to properly define the settings of the models and boundary conditions in order to achieve reliable results. In addition, it is recommended to include in the simulations the different systems, such as the cooling and the engine oil lubrication systems, to replicate realistic conditions. However, the computational domain becomes then very large, and the computational time needed for the calibration phase and the convergence grows dramatically [36]. Thus, simplified approaches tend to be used to optimize the calculation time. Commonly the systems are simulated independently; for example the cooling and oil refrigeration systems are not considered in the CHT calculations when the combustion is modelled. In this case it is important to set accurate boundary conditions in the regions adjacent to the systems not considered in the computational domain. However, it is often challenging to estimate experimentally boundary conditions for the

engines parts, such as the piston rings and the piston oil cavity. Empirical correlations available in the literature may be used [37], but they have uncertainties that may need additional tuning steps.

Though experimental measurements are more accurate to estimate the heat flux in ICEs [38], they imply a high economical cost. Hence, the automobile industry has a special interest in developing engineering tools that allow predicting the heat losses in ICEs. As commented above, a good strategy that combines accuracy and optimization of resources is the use of coupled 1D-3D models to study the heat transfer in ICEs.

In this framework, a methodology for the thermal prediction in the solid components of an ICE is presented in this paper. The approach employs a 1D model integrated with 3D discretized elements to determine the heat transfer through the combustion chamber walls and estimate the wall temperatures in the solid domain of the engine. The latter may then be used as accurate boundary conditions in a 3D CHT simulation to accelerate the calibration process of the engine and produce precise heat losses results.

This study was performed in a single cylinder gasoline direct injection engine, including the cooling and the oil refrigeration systems. Furthermore, the results are compared with the experimental data available. This paper is divided in 5 main sections. In section 2 the methodology employed to estimate the temperature field of the components is described in detail. Section 3 presents the 1D numerical model integrated with 3D elements of the engine structure. In section 4 the results are compared with experimental data from the engine, and a heat transfer analysis to determine the suitability of the approach is presented. Finally, in section 5 the conclusions of this study and its convenience to predict the heat transfer and estimate temperatures for the solid domain are presented.

2. Methodology

The commercial multi-physics CAE (Computer Aided Engineering) system simulation GT-SUITE [39] has been used for developing the methodology employed in this work. This approach is based on solving the flow regions by 1D modelling, while the solid components of the engine are calculated by 3D FEA modeling. The thermal distribution obtained in the solid regions will allow to determine boundary conditions for the CHT solid domain. The methodology can be separated in two main parts: on the one hand, the validation of the 1D engine model; on the other hand, the validation of the 3D integrated thermal model. The methodology followed to carry out the simulations is summarized in Fig. 1.
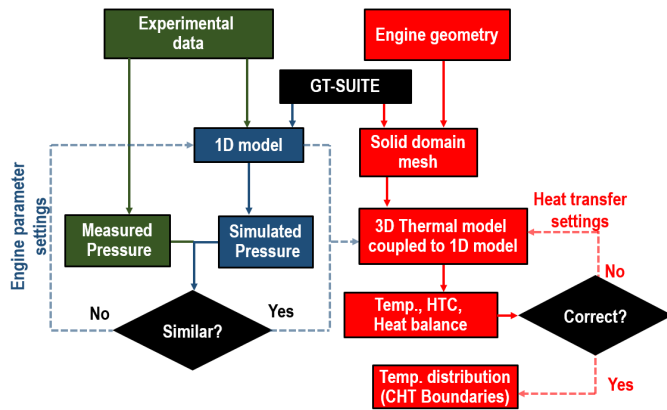

Figure 1: Methodology employed for the calculations.

2.1. 1D engine model

For describing the engine fluid domain, a 1D multi-physics model of the GT-SUITE commercial software was employed. A complete 1D wave action model layout (shown in Fig. 2) of the experimental facility, including the single cylinder engine, was generated after gathering the required geometric information of the different elements, as described in section 3.1. The approach was employed to perform a full cycle calculation of the engine considering the intake and exhaust stages, as well as the combustion process.

For the combustion process simulation, a Heat Release Rate (HRR) profile was imposed in the cylinder coming directly or indirectly, after a proper scaling, from thermodynamic analysis of the experimental instantaneous cylinder pressure. For this simulation the walls in contact with the gas were assumed as isothermal and the heat transfer through the solid components of the engine was not taken into account. In order to achieve good results, the engine flow domain had to be modeled properly, and the engine 1D model verified. In this regard, a validation by comparison of the experimental and simulated in-cylinder pressure traces was carried out as done by [40]. About 40 engine cycles were required to converge the simulation and thus verify the validity of the engine model.

2.2. 3D integrated thermal model

On the other hand, the GT-SUITE 3D program was used to build a FEA mesh for the solid components of the engine geometry (piston, cylinder block, head and valves) in the 3D space, and create a thermal model that included also the interaction with the cooling and oil systems [32]. The thermal model, described in detail in section 3.2, was coupled to the flow domain of the 1D engine model, so that the convective properties of the gas calculated with the 1D model were employed as boundary conditions for the 3D thermal model. Validation of the coupled model had to be verified by renewed comparison of the simulated pressure traces with the experimental data and iterations performed until convergence.

Finally, the thermal model results showed the heat transfer balance and distribution in the various engine solid parts. Once converged, this permitted to perform a heat transfer analysis and calculate the accurate temperature distribution in the solid engine components. The surface temperatures could then be employed as boundary conditions for more complex models, such as CFD-CHT.

3. Description of models

3.1. Engine model

The geometry of a SI engine provided by IFP Energies Nouvelles (IFPEN) was used in this work, with the engine specifications given in Table 1. The domain was simplified in the 1D model considering the intake/exhaust ports and

valves along with the combustion chamber walls. The diameter and length of the pipes were determined by measuring the CAD (Computer-aided design) of the real geometry. Table 1 also shows the details about the operation point used for the simulations. Furthermore, Fig. 2 displays the 3D engine geometry and its simplified 1D model.

Table 1: Engine specifications.

Engine type	4-stroke spark ignited
IMEP [bar]	7
Engine speed [rpm]	3000
Ignition timing [cad aTDC]	-27
Bore - Stroke [mm]	75-93
Compression ratio	14:1
Number of valves [-]	2 intake and 2 exhaust

As mentioned in section 2.1, the walls in contact with the flow were considered as isothermal and obtained from a lumped model [13, 41]. The pressure and temperature boundary conditions in the intake and exhaust ports were imposed according to the measured experimental values. In order to model properly the intake and exhaust flow ratio the experimental discharge coefficients were set as boundary conditions in the engine valves, while the ports were modeled with no friction pressure losses. In addition, the Colburn correlation [42] was used for the heat transfer through the walls.

To simulate the injection process the fuel mass and the instantaneous injection pressure were imposed during the injection timing. The injection pressure trace is displayed in Fig. 3. It was obtained from a previous CFD simulation with the computational software CONVERGE [37].

As allowed by the software, the CAD geometry of the engine was introduced in the GT-SUITE model. With this, the combustion process could be better modeled. The spark location in the combustion chamber was also defined. A predictive combustion model with standard Laminar Flame Speed and Turbulent Flame Speed models was used to solve the combustion process. Finally, the model was calibrated by adjusting mainly the Flame Kernel Growth multiplier, Turbulent Flame Speed Multiplier and the Taylor Length Scale Multiplier.
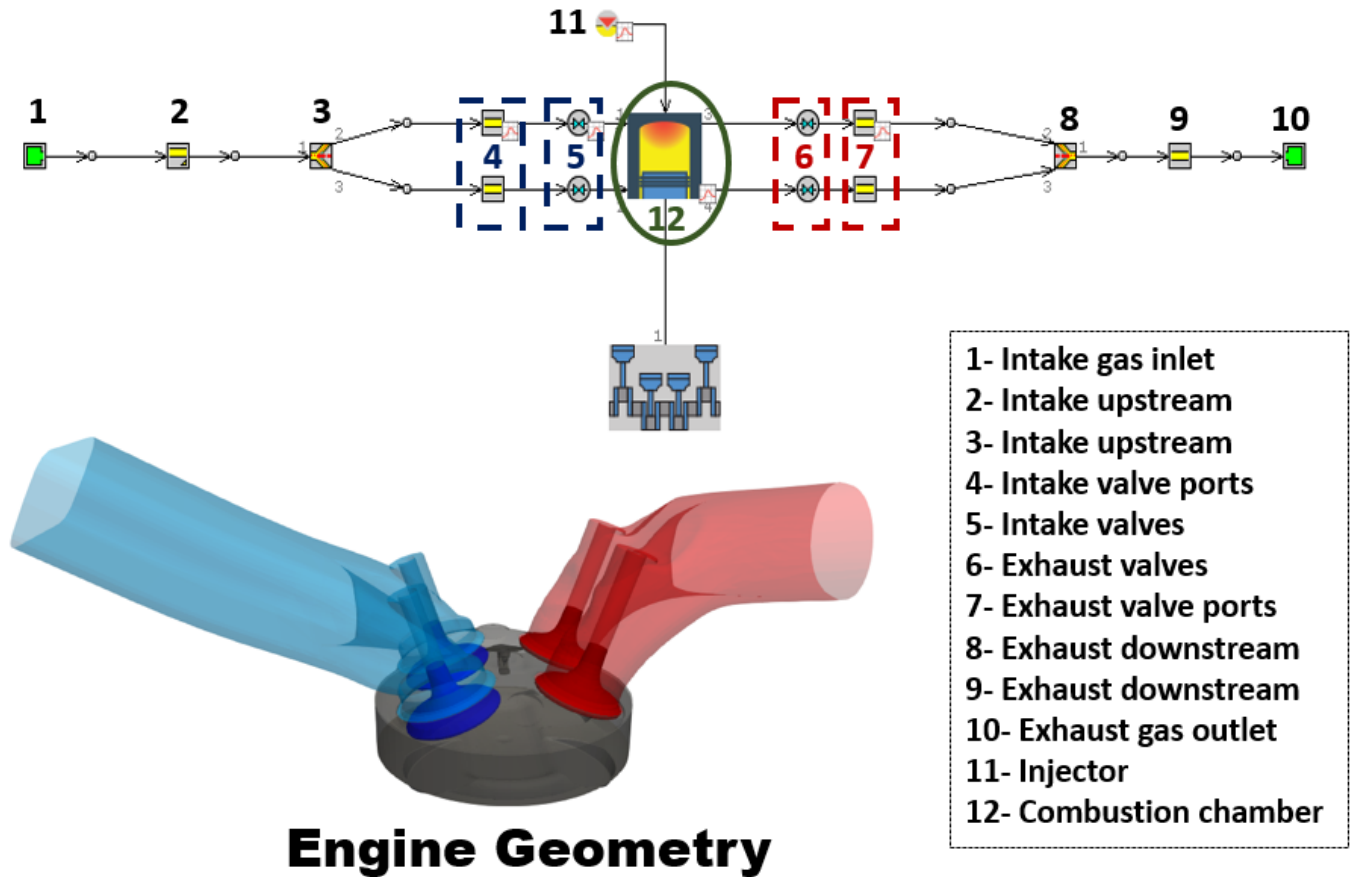

1- Intake gas inlet
2- Intake upstream
3- Intake upstream
4- Intake valve ports
5- Intake valves
6- Exhaust valves
7- Exhaust valve ports
8- Exhaust downstream
9- Exhaust downstream
10- Exhaust gas outlet
11- Injector
12- Combustion chamber

Engine Geometry

Figure 2: 1D Engine model.

In the combustion chamber (12 in Fig. 2) the WoshniGT heat transfer model [39] was used with an overall convection multiplier of 1.13 with head/bore and piston/bore area ratio obtained from the 3D geometry.

Finally, to solve the ordinary differential equations, a Skyline Matrix Sparse Format solver with the Cuthill-McKee matrix optimization method was used [43], along with an Explicit Runge-Kutta algorithm.
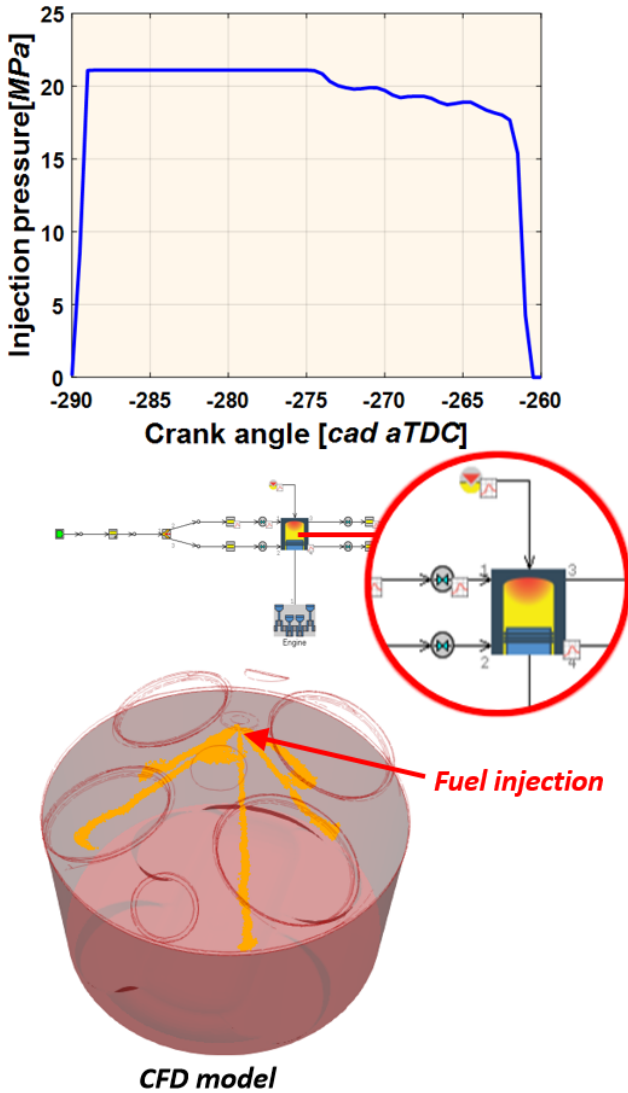

Figure 3: Injection pressure during the engine cycle.

3.2. 3D Thermal model

The full thermal model is shown in Fig. 4. As mentioned above, in this model the oil and the coolant systems were considered for the simulations. The oil composition and the volumetric flow rates were the inputs for the block

and the head of the oil coolant system. A shaped flow volume was used to define the surfaces of the engine in contact with the oil where the volume and the surfaces areas needed to be specified. The Colburn correlation was used for the heat transfer with a friction multiplier equal to 1.In addition, the characteristic length and the expansion diameter had to be considered for this fluid volume. This part was attached to the engine structure by a convective heat transfer coefficient variable (30 and 31 in Fig. 4). A motor oil SAE 5W-30 was considered for the oil circuit.

The engine coolant system was formed by the block and head coolant jacket, which were connected by orifices with adjacent diameters given by the CAD of the geometry (10,11, 12, 13 in Fig. 4). Both components included the inlet and the outlets of the coolant circuit as shown in Fig. 4. In this single cylinder engine one inflow pipe was defined in the block coolant jacket (7 in Fig. 4), while the head coolant jacket was modeled with two outflow pipes (17 and 20 in Fig. 4). Again, for both flow volumes the Colburn heat transfer correlation was considered, with the same friction multiplier used for the oil system. GT-SUITE calculates the convective properties of the fluid with flow rate and inlet/outlet temperatures, and uses them as boundary conditions to calculate the solid domain. In addition, the angles with respect to X, Y and Z were determined for all orifices of the 3D volumes. The inlet/outlet temperatures and flow rate were imposed as boundary conditions in the model, based on the experimental data. The "egl-5050" fluid from the GT-SUITE library was used as engine coolant, due to its similarity to the experimental refrigerant. Fig. 5 shows a simplified scheme of the engine cooling system.

As mentioned in section 2.2, a finite element representation of the different parts of the ICE was employed to model the solid components of the engine: cylinder block, liner, piston, head and valves. The solid domain of the FE structure was formed by 431926 cells, 103207 nodes and 42 boundaries. Due to their size, the engine head and the cylinder block took up most of the cells, as shown in Table 2. The meshed computational domain is displayed in Fig. 6.

Every component of the engine required the definition of boundary conditions for the heat transfer model. Gas boundary conditions were specified for the head, the intake and exhaust manifold, and for the combustion gas exposed surfaces. In addition, solid contact boundary conditions were used in the parts of the head in contact with the four valves (seats and guides). In the engine cylinder block the height of the liner exposed to the gas above the piston at bottom dead center (BDC) and the height exposed to the oil below piston at top dead center (TDC) were defined. The piston was divided into several parts as indicated in Fig. 7: ring, crown, contact oil, skirt and piston surface exposed to the gas. Finally, a custom element mesh was
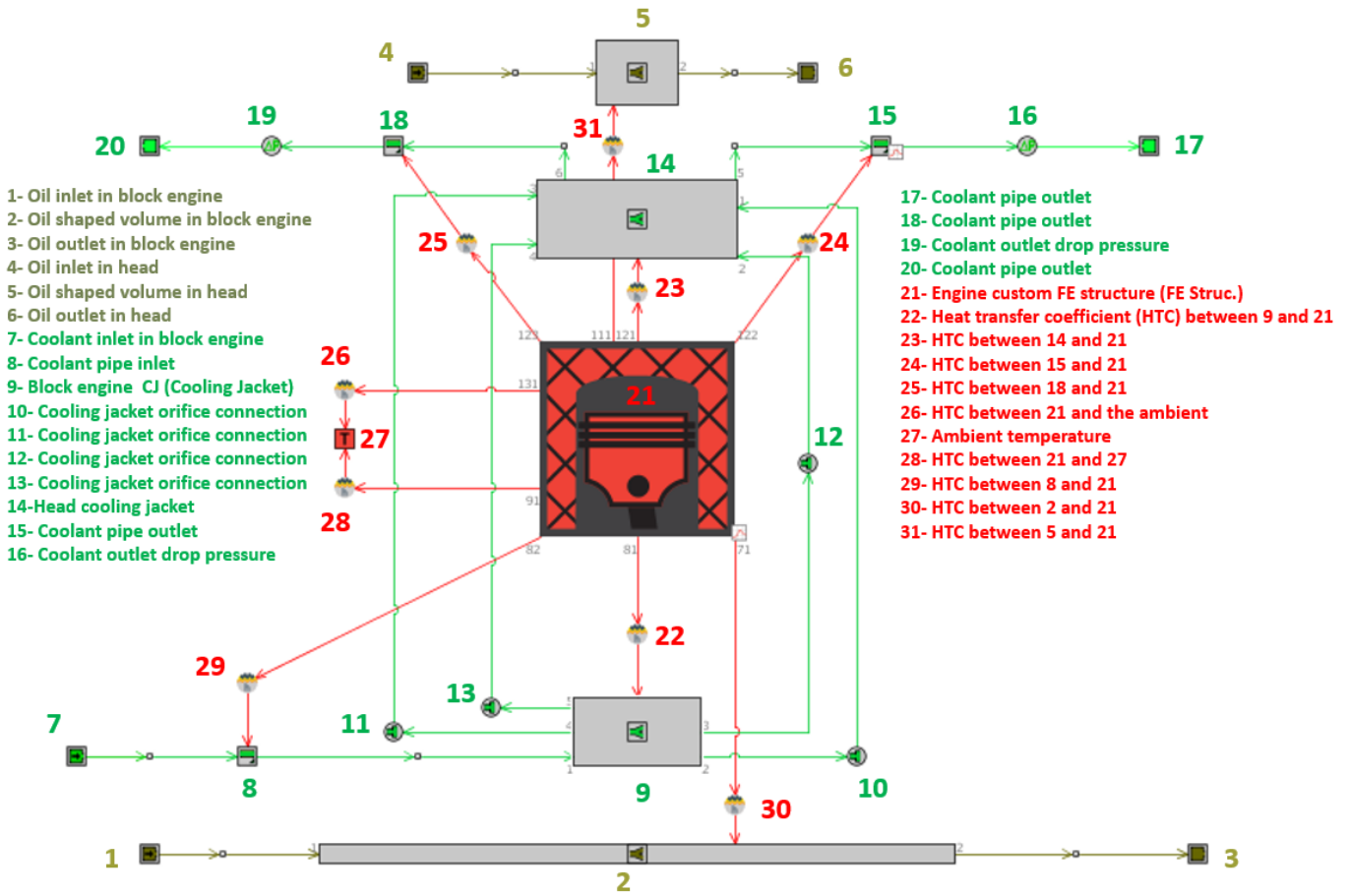
Figure 4: Thermal model with integrated 3D FE structure.

1- Oil inlet in block engine
2- Oil shaped volume in block engine
3- Oil outlet in block engine
4- Oil inlet in head
5- Oil shaped volume in head
6- Oil outlet in head
7- Coolant inlet in block engine
8- Coolant pipe inlet
9- Block engine CJ (Cooling Jacket)
10- Cooling jacket orifice connection
11- Cooling jacket orifice connection
12- Cooling jacket orifice connection
13- Cooling jacket orifice connection
14- Head cooling jacket
15- Coolant pipe outlet
16- Coolant outlet drop pressure

17- Coolant pipe outlet
18- Coolant pipe outlet
19- Coolant outlet drop pressure
20- Coolant pipe outlet
21- Engine custom FE structure (FE Struc.)
22- Heat transfer coefficient (HTC) between 9 and 21
23- HTC between 14 and 21
24- HTC between 15 and 21
25- HTC between 18 and 21
26- HTC between 21 and the ambient
27- Ambient temperature
28- HTC between 21 and 27
29- HTC between 8 and 21
30- HTC between 2 and 21
31- HTC between 5 and 21

used for the intake/exhaust valves, with given location and normal orientation in space. The material for the head, piston and cylinder block engine was defined as aluminum 2024-T6, while for the valves it was carbon steel.

When performing the simulations each part of the solid domain was uniformly initialized with the corresponding average wall temperature used in the 1D model to solve the fluid domain. Then, the new convective boundary conditions were employed to calculate by FEA the temperature distribution in the solid. Finally, the convergence of the full integrated domain was achieved when there were no more cycle to cycle variations.
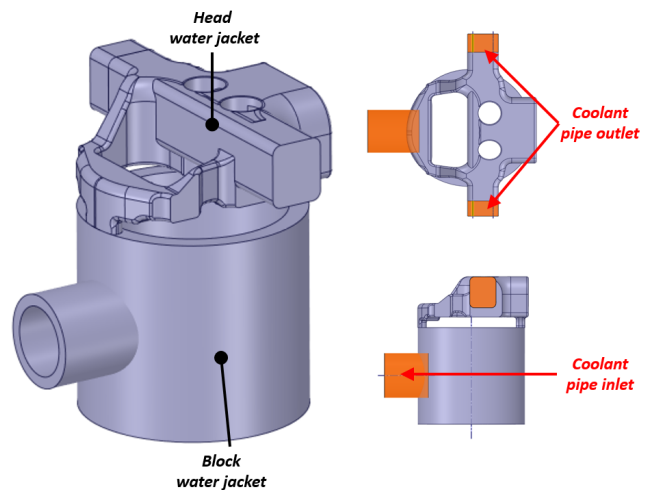

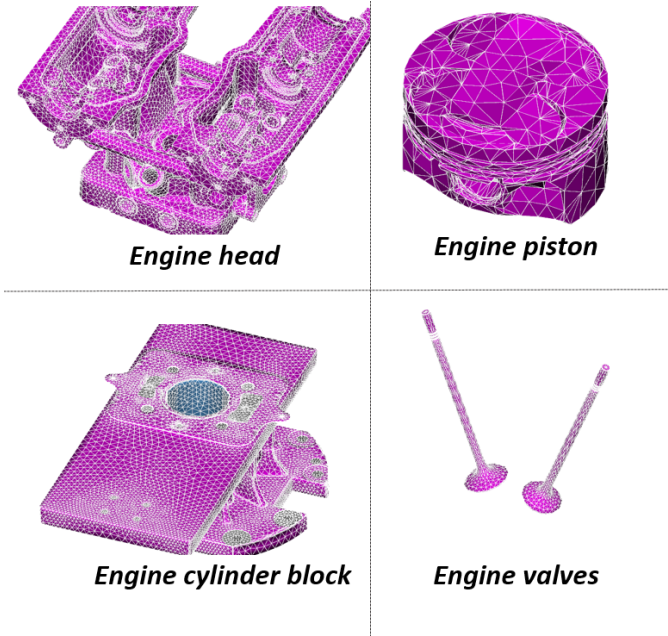Figure 5: Scheme of the 3D cooling circuit of the engine

6

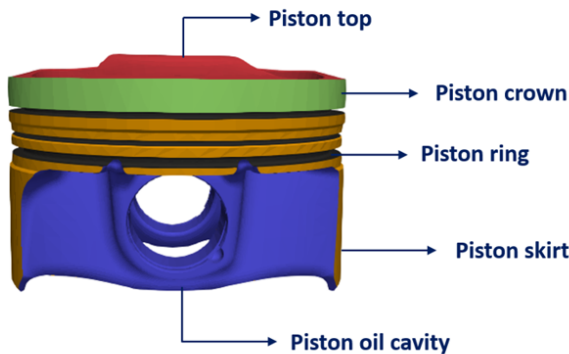Figure 6: Meshed computational domain employed for the FIM.

Figure 7: Piston regions considered in the computational domain [37].

Table 2: 3D Mesh data of the thermal model.

FE element	Nodes	Cells	Boundaries
Head	47859	194199	22
Intake Valves	1567	5701	4
Exhaust Valves	1489	5383	4
Piston	2223	8039	6
Cylinder block	50069	226632	6
Total	103207	431926	42

4. Results and discussion

This section presents the most important results obtained with the above described approach. In order to evaluate the accuracy of the 1D-3D fully integrated model (1D-3D FIM), the simulated results were compared with available experimental data for the studied ICE. In addition, a thermal analysis was carried out for the solid engine parts.

4.1. Combustion validation

The 1D engine model was initially calibrated considering isothermal walls. By integrating the FE structure in the model, the heat transfer inputs and the boundary conditions changed. This new model had to be validated also. The pressure traces obtained with the simple 1D model on the one hand, and with the 1D-3D FIM on the other hand, are compared to the experimental data in Fig. 8. The experimental in-cylinder pressure was measured with convectional sensors and more details about the experiment can be found in [44].
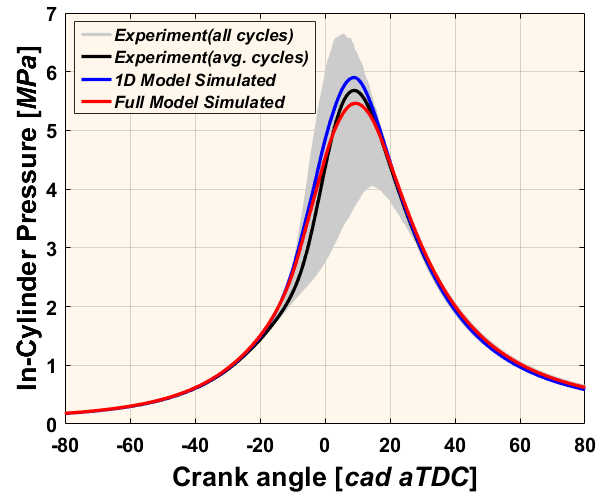

Figure 8: Calculated and measured in-cylinder pressure traces.

The pressure trace of the 1D decoupled model (blue line) is over-predicted with respect to the mean experimental one (black line), with a maximum difference of 3.9 % (2.2 bar). On the contrary, the simulated in-cylinder pressure obtained with the coupled model (red line) is under-predicted by about 3.9 % (2.2 bar) also at peak pressure. However, the calculated values with both approaches (1D-model and 1D-3D FIM) fall within the experimental dispersion of the measurements, represented by the grey shadowed area on Fig. 8.

Cycle-to-cycle variations (CCV) between successive combustion events are often present in SI engines [45] as indicated in the literature [46, 47] and they occur due to variances in the burn rate for each consecutive cycle

7

[48]. In this regard, the GT-SUITE combustion model is not able to predict the cyclic dispersion that characterizes SI engines, so that only the average in-cylinder pressure trace (black line) can be considered as reference for the comparison.

4.2. Heat transfer analysis

To determine the suitability of the approach to evaluate the heat transfer in the engine, a heat transfer analysis was performed. Fig. 9 shows the comparison of the calculated values of temperature and heat transfer coefficient (HTC) of the gas in the combustion chamber with values determined from experimental conditions by an in-house predictive calculation tool [41, 49]. Both traces have similar trends and values during the combustion process. The 3D-FIM temperature is higher for most of the cycle. However, the trend is not so clear for the HTC, which is higher for the experimental one before TDC and lower during the expansion stroke. The figure shows a lag between the two HTCs. This difference may be due to the fact that the combustion chamber is simplified to a 1D model in the 3D-FIM approach.
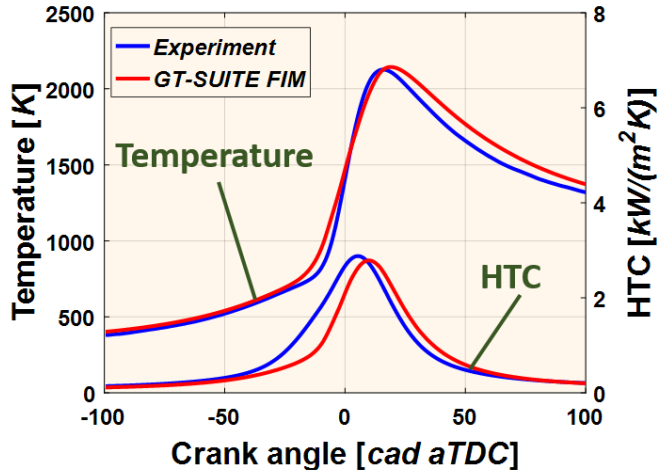

Figure 9: In-Cylinder gas temperature and heat transfer coefficient (HTC).
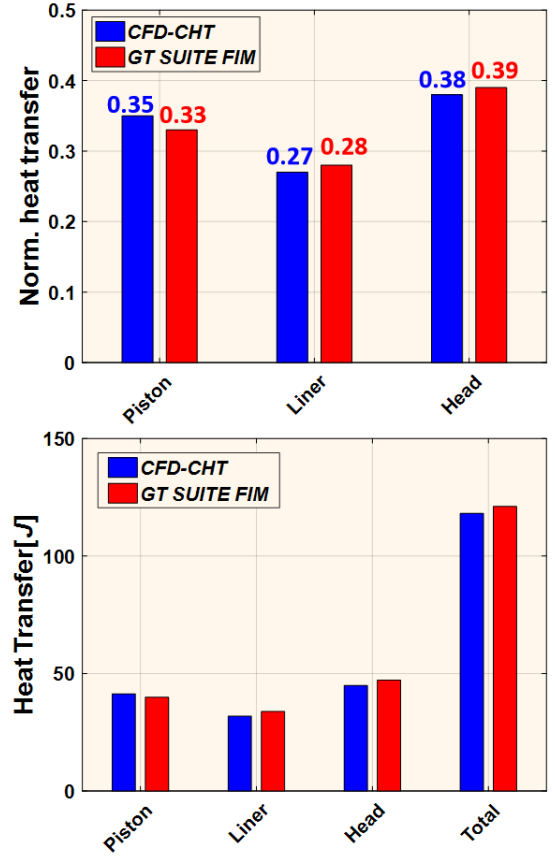

Figure 10: Normalized heat transfer (top) and heat transferred (bottom) through the combustion chamber walls.

To better understand these differences, the heat balance was compared with that obtained with a CFD-CHT simulation of the same engine, whose results were validated with the experimental data available [35]. The comparison is presented in Fig. 10. Higher total heat transfer is observed in the results of the 3D-FIM model. When considering the heat transfer through the components walls, the 3D-FIM model yields higher values for the cylinder head and liner than the CFD-CHT. On the contrary, the heat transferred through the piston is higher in the CFD-CHT case. However, it is remarkable that the heat transfer distribution through the combustion chamber walls is similar for both models, with the highest difference observed in the piston. The differences in the heat balance between both models are presented in Table 3. The percentage error was determined by equation 1:

$$\text{Error} = \left(1 - \frac{x_{ref}}{x_{1D-3D}}\right) 100 \qquad (1)$$

where x_{ref} is the variable related to the reference value (CFD-CHT), while x_{1D-3D} is referred to the 1D-3D FIM.

Table 3: Heat transferred through the combustion chamber walls.

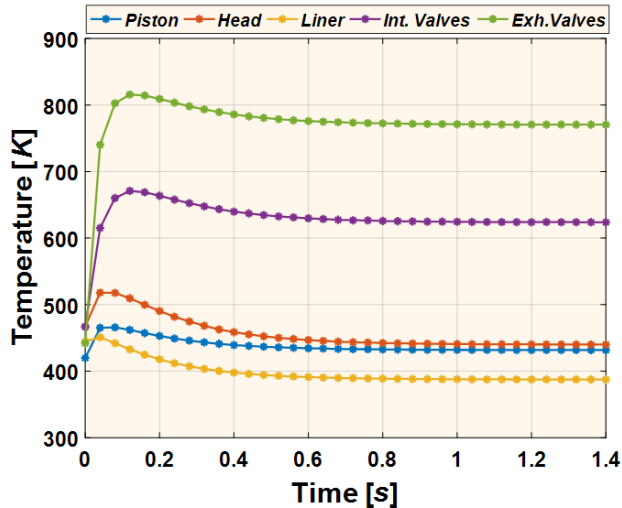| Wall	CFD-CHT [J]	GT-SUITE [J]	Diff [%]
Piston	41.34	39.96	3.32
Liner	31.89	33.91	-6.34
Head	44.88	47.23	-5.24
Total	118.10	121.10	-2.54

Figure 11: Convergence of the temperatures at the gas exposed surfaces in the combustion chamber.

4.3. 3D FE engine components thermal analysis

The temporal evolution of the temperatures at the surfaces of the various engine components exposed to the combustion gas are plotted in Fig. 11, as these are bound to be the hottest walls. All the solid surfaces of the engine reached steady state very quickly, after about 0.6 seconds. Clearly, the surface temperatures are very different in each component. The hottest temperature (about 770 K) is reached in the carbon steel exhaust valves, followed by the intake valves (about 620 K). The piston top and the head surface converge at a very similar temperature of about 450 K, while the liner remains at the coolest temperature of about 390 K. The significant temperature difference between the valves and the rest can be explained by the different thermal properties of the materials, and by the cooling of the piston and head.

The temperature distribution in the various solid parts of the engine are analysed next. Figures 12 to 14 show the spatial distribution of the temperature on the various engine components.

As expected, the surface exposed to the gas is the hottest wall of the cylinder head (Fig. 12). The temperature distribution on this surface shows that the highest temperatures are located near the exhaust ports. These are refrigerated internally by the cooling liquid, and hence, the temperature is getting lower at the exhaust outlet. The

coldest parts of the solid head are located at the inlet of the intake manifold in the regions exposed to the ambient and the cooling oil. Finally there is a significant temperature difference of about 120 K between the hottest (473 K) and the coolest parts (356 K).
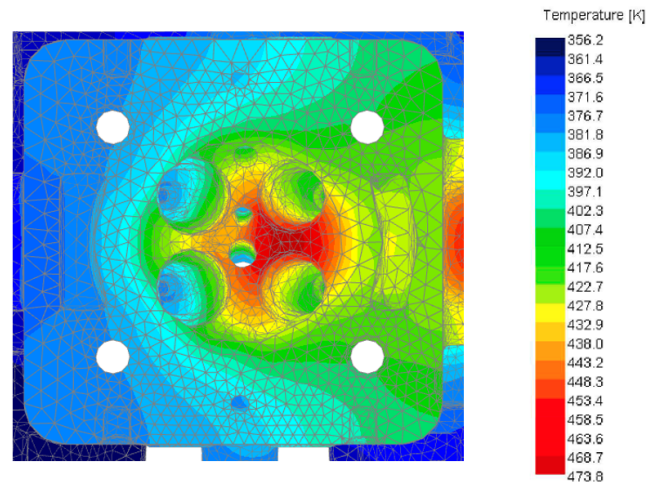

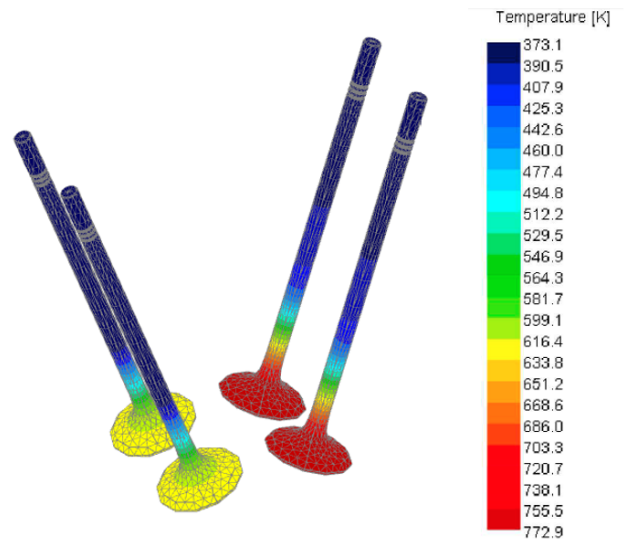Figure 12: Temperature distribution in engine head.

Figure 13: Temperature distribution in engine valves.

Fig. 13 shows the temperature distribution in the four engine valves. The two intake valves have exactly the same distribution and the surfaces in contact with the combustion gas have the highest temperatures reaching up to 625 K. The maximum temperature difference is of the order of 250

K, with a minimum temperature of about 373 K in the valve guides. The two exhaust valves also present identical temperature distribution, where the hottest surface (773 K)is the one in contact with the chamber gas and the coldest (373 K) is in the guide valves. In this case the highest temperature difference is about 400 K.
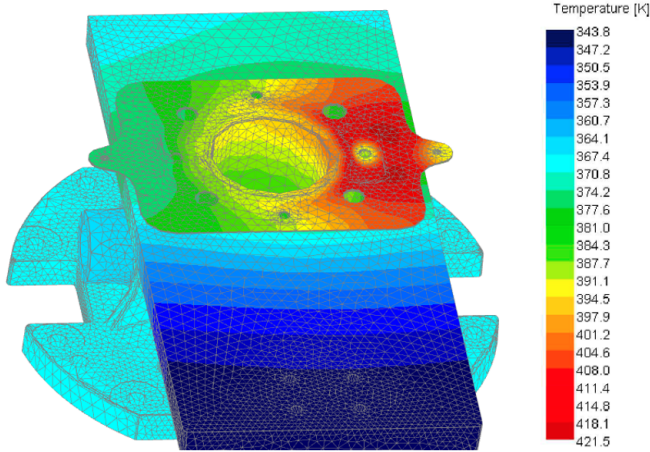
case, the maximum temperature value on the engine piston is approximately 440 K, while the minimum is about 382 K, i.e the lowest temperature difference of all components, about 60 K.
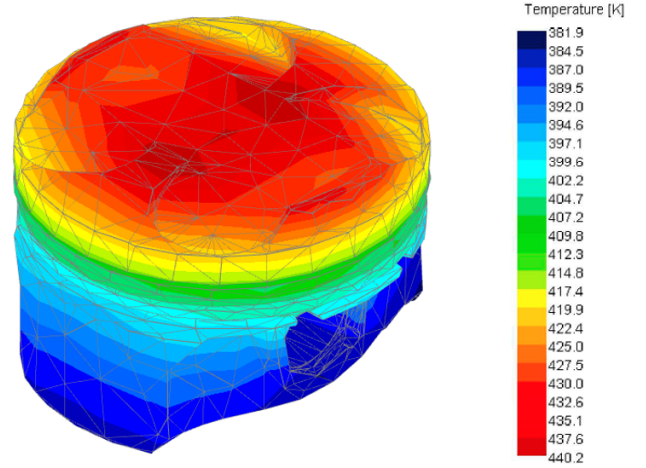

Figure 14: Temperature distribution in engine cylinder.

Figure 15: Temperature distribution in engine piston calculated with FIM model.

The spatial temperature distribution in the engine cylinder is shown in Fig. 14. The hottest regions are located in the liner part closest to the head, which is part of the combustion chamber. The coolest regions are the surfaces exposed to the ambient and closer to the inlet of the coolant jacket. The maximum temperature difference in this component is about 80 K, with the highest in the domain reaching 422 K and the lowest at 344 K.

The engine piston is one of the most complex parts of an ICE in terms of heat transfer. Indeed, it moves during the cycles and it is surrounded by several fluids, such as the coolant oil and the combustion gas. In addition, the piston is provided with segment rings, which transfer heat by means of mechanical friction due to the movement. This friction was modeled using standard values of the software [39]. Fig. 15 shows that the spatial temperature distribution on the piston is in good agreement with some literature results[36, 50]. The hottest wall is the gas exposed surface, while the coldest walls are in the coolant oil cavity. Similar results in spatial temperature distribution have been found with full CFD-CHT calculations [37]. However, due to the simplifying assumptions made for the 1D models described in this work, some local effects such as hot spots on the surfaces cannot be predicted with the same accuracy as the full 3D CFD-CHT. Nonetheless, the 1D-3D FIM allows estimating mean temperature values on the surfaces. In this

The results obtained for the piston of the SI engine with the 1D-3D FIM are compared with the solution of a full 3D calculation, where CHT was applied to the same solid piston and for the same operation point. This calculation was performed with the program CONVERGE and with settings previously used in CHT simulations of the same engine [37]. In order to set adequate boundary conditions, the piston was divided in five parts also, as indicated in Fig. 7. Boundary conditions for the piston ring, skirt and oil cavity were estimated from literature correlations. The spatial temperature distribution in the solid piston obtained with the CHT is shown in Fig. 16. As may be observed, the temperature distribution is very similar and of the same order of magnitude as the one calculated with the 1D-3D FIM (Fig. 15).
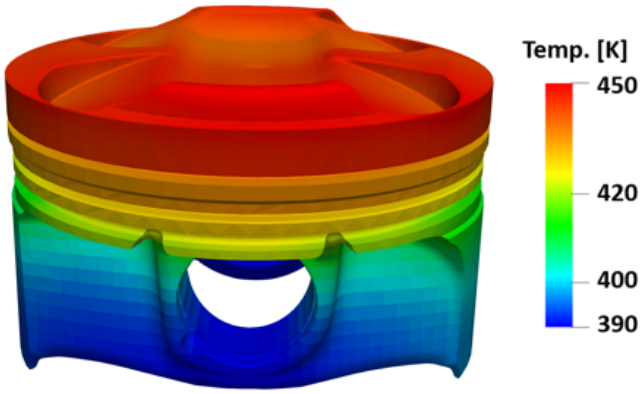
Figure 16: Temperature distribution in the solid piston calculated with full CFD-CHT simulation.

The experimental engine volumetric, combustion and indicated efficiencies were calculated using the experimental data [44] with the following expressions:

Volumetric efficiency

$$\eta_{\mathrm{vol}} = \frac{m_{air}}{\rho \cdot V_T} \cdot 100 \qquad (2)$$

where m_{air} is air mass filled into the combustion chamber at IVC, ρ is the density of the air upstream and V_T is the maximum volume of the cylinder.

Combustion efficiency [51]

$$\eta_{\mathrm{comb}} = \left(1 - \frac{m_{HC}}{m_{\mathrm{fuel}}} - \frac{m_{CO}}{4 \cdot m_{\mathrm{fuel}}}\right) \cdot 100 \qquad (3)$$

where m_{HC} represents the mass of unburned HC emissions, m_{CO} is the mass of CO and m_{fuel} is the injected fuel mass.

Indicated efficiency

$$\eta_{\mathrm{in}} = \frac{W}{m_{\mathrm{fuel}} \cdot Cp} \cdot 100 \qquad (4)$$

where W is the indicated work of the engine, and Cp is the calorific power of the fuel.

Finally, the errors between the experimental and the 1D-3D FIM efficiencies were calculated with equation 1, were x_{ref} is referred to the experimental values.

Table 5 presents the experimentally estimated engine efficiencies and those obtained with the 1D-3D FIM. It shows differences of 6.2 %, 1.8 % and 4.0 % in the volumetric, combustion and indicated efficiencies respectively. The major difference between both models is on the volumetric efficiency. This may be due to several reasons that may affect the 1D-3D FIM results: the simplified meshing of the intake pipes, the values of the discharge coefficients that may not be very accurate, and some differences in the combustion chamber volume due to the 1D simplification. Nonetheless, the tolerance is acceptable, considering that the SI engine has some significant experimental dispersion that cannot be estimated by the model.

To further illustrate the similarity of the results, the average temperatures calculated with both models in the different piston regions are compared in Table 4. In the 1D-3D FIM these values are determined by averaging the spatial temperature distribution on each surface.

Clearly, both models yield very similar results with a maximum difference in temperature of less than 5% at the piston ring. Due to the friction between the piston and the liner, it is possibly the most complicated region of the piston. To define accurately the boundary conditions in this zone, more advanced tribology models may be required.

Though both models show very similar results, the calculation times are significantly different. In the case of the CFD-CHT, several cycles iterations are necessary to converge the model and further calibration settings in the solid region may be necessary at each cycle. Hence, these calculations take several days, or even weeks depending on the processors available. By comparison, the fully integrated model allows obtaining a spatial temperature distribution in a few minutes only. However, when the full CFD-CHT simulation is necessary, the 1D fully integrated model presented here may provide accurate thermal boundary conditions for the diverse solid parts of the engine. This would help save significant calibration and computing time.

Table 4: Boundary conditions on piston for CHT calculations.

Solid surface	1D-3D model Avg. T [K]	CHT model Avg. T [K]	Percentage error [%]
Piston top	429.7	433.3	0.9
Piston crown	426.1	432.8	1.5
Piston skirt	401.7	409.2	1.8
Piston ring	396.5	414.1	4.3
Piston oil	398.6	405.9	1.8

Table 5: Engine efficiencies.

	Exp. [%]	GT-SUITE [%]	Diff [%]
Vol. efficiency	77.0	81.8	6.2
Comb. efficiency	96.3	98.0	1.8
Ind. efficiency	43.0	41.3	4.0

4.4. Engine efficiencies

5. Conclusions

Accurate prediction of the heat transfer in a combustion engine is of great interest nowadays to help improve its thermal efficiency. For this it is important to consider all the systems included in the engine, such as the cooling and oil refrigeration circuits.

3D CFD-CHT numerical approaches appear to be one of the most useful tools to predict the heat transfer in ICEs. However, they are quite complex to set up and require excessively long computational times, which renders them quite costly. For this reason, the cooling systems are usually not included in the calculations, replaced instead by estimated boundary conditions based on empirical relations, that may not be accurate enough.

In this paper a fully integrated 1D-3D new approach (FIM) has been presented that allows calculating the heat transfer and the temperature distribution in the various solid engine elements accurately and very rapidly. The methodology couples the fluid and solid regions by solving the gas flow in the engine by 1D modelling and the solid components with a 3D FEA. Moreover, the coolant jacket and the oil for the refrigeration of the head and the engine cylinder block are also taken into account, so that more accurate results can be obtained. These coupled calculations take only a few minutes once the model has been properly calibrated.

First, the FIM model has been validated against experimental measurements, proving that the in-cylinder pressure trace obtained is within the experimental dispersion of the engine. Then the approach has been employed to calculate the heat transfer through the combustion chamber walls and the temperature distribution in all the solid parts of the engine, such as the head, the intake/exhaust valves, the piston and the cylinder block. The results of the heat transfer analysis thus estimated have been compared with the ones obtained from an accurate CFD—CHT simulation and a maximum difference of about 6% has been observed between both methods.

Moreover, very good agreement between both methods has been found in terms of spatial wall temperature distribution on the piston. Hence, the results presented in this work suggest that the 1D-3D FIM methodology may be of great advantage at design stage to estimate rapidly the heat transfer through the different engine components, and the wall temperature distribution in the solid parts with accuracy.

Additionally, the temperature distributions calculated for the engine components can be employed to define well-estimated boundary conditions for more complex and accurate CFD-CHT calculations, which are sometimes necessary. Indeed, though this type of 3D simulation tends to be costly, it is particularly useful to study local thermal effects which might produce knock in the SI engine. And also to assess the transient evolution of the temperature in engines insulated with some smart coating of the kind used to reduce heat losses. This is not possible with the steady state approach described in this paper.

Finally, the engine efficiencies predicted by the 1D-3D FIM model are reasonably close to the experimental values, especially considering all the simplifications made in the 1D-3D FIM. However, in future work, it may be interesting to develop a more advanced and complex model to help increase the accuracy of the FIM results.

References

[1] M. Weiss, P. Bonnel, J. Kühlwein, A. Provenza, U. Lambrecht, S. Alessandrini, M. Carriero, R. Colombo, F. Forni, G. Lanappe, et al., Will euro 6 reduce the nox emissions of new diesel cars?– insights from on-road tests with portable emissions measurement systems (pems), Atmospheric Environment 62 (2012) 657–665. doi:https://doi.org/10.1016/j.atmosenv.2012.08.056.

[2] M. Leguille, F. Ravet, J. Le Moine, E. Pomraning, K. Richards, P. K. Senecal, Coupled fluid-solid simulation for the prediction of gas-exposed surface temperature distribution in a si engine, WCX™ 17: SAE World Congress Experience (mar 2017). doi: https://doi.org/10.4271/2017-01-0669.

[3] M. C. Parker, C. Jiang, D. Butcher, A. Spencer, C. P. Garner, D. Witt, Impact and observations of cylinder deactivation and reactivation in a downsized gasoline turbocharged direct injection engine, International Journal of Engine Research (2019) 1468087419882817. doi:https://doi.org/10.1177/1468087419882817.

[4] S. B. Shrestha, G. A. Karim, Hydrogen as an additive to methane for spark ignition engine applications, in: IECEC-97 Proceedings of the Thirty-Second Intersociety Energy Conversion Engineering Conference (Cat. No. 97CH6203), Vol. 2, IEEE, 1997, pp. 910–915.

[5] X. Yu, H. Wu, Y. Du, Y. Tang, L. Liu, R. Niu, Research on cycle-by-cycle variations of an si engine with hydrogen direct injection under lean burn conditions, Applied Thermal Engineering 109 (2016) 569–581.

[6] N. Iafrate, M. Matrat, J.-M. Zaccardi, Numerical investigations on hydrogen-enhanced combustion in ultra-lean gasoline spark-ignition engines, International Journal of Engine Research (2019) 1468087419870688. doi:https://doi.org/10.1177/1468087419870688.

[7] H. Kosaka, Y. Wakisaka, Y. Nomura, Y. Hotta, M. Koike, K. Nakakita, A. Kawaguchi, Concept of "temperature swing heat insulation" in combustion chamber walls, and appropriate thermo-physical properties for heat insulation coat, SAE International Journal of Engines 6 (1) (2013) 142–149. doi:https://doi.org/10.4271/2013-01-0274.

[8] A. Kikusato, K. Terahata, K. Jin, Y. Daisho, A numerical simulation study on improving the thermal efficiency of a spark ignited engine — part 2: Predicting instantaneous combustion chamber wall temperatures, heat losses and knock —, SAE International Journal of Engines 7 (1) (2014) 87–95. doi:https://doi.org/10.4271/2014-01-1066.

[9] Y. Wakisaka, M. Inayoshi, K. Fukui, H. Kosaka, Y. Hotta, A. Kawaguchi, N. Takada, Reduction of heat loss and improvement of thermal efficiency by application of "temperature swing" insulation to direct-injection diesel engines, SAE International Journal of Engines 9 (3) (2016) 1449–1459. doi:https://doi.org/10.4271/2016-01-0661.

[10] E. Gingrich, M. Tess, V. Korivi, P. Schihl, J. Saputo, G. Smith, S. Sampath, J. Ghandhi, The impact of piston thermal barrier coating roughness on high-load diesel operation, International Journal of Engine Research (2019) 146808741989348. doi:https://doi.org/10.1177/1468087419893487.

[11] J. Somhorst, M. Oevermann, M. Bovo, I. Denbratt, Evaluation of thermal barrier coatings and surface roughness in a single-cylinder light-duty diesel engine, International Journal of Engine Research (2019) 1468087419875837. doi:https://doi.org/10.1177/1468087419875837.

[12] H. Yu, W. Su, Numerical study on the approach for super-high thermal efficiency in a gasoline homogeneous charge compression ignition lean-burn engine, International Journal of Engine Research (2019) 1468087419889248. doi:https://doi.org/10.1177/1468087419889248.

[13] A. Torregrosa, P. Olmeda, B. Degraeuwe, M. Reyes, A concise wall temperature model for di diesel engines, Applied Thermal Engineering 26 (11-12) (2006) 1320–1327.

[14] A. Torregrosa, P. Olmeda, J. Martín, B. Degraeuwe, Experiments on the influence of inlet charge and coolant temperature on performance and emissions of a di diesel engine, Experimental Thermal and Fluid Science 30 (7) (2006) 633 – 641. doi:https://doi.org/10.1016/j.expthermflusci.2006.01.002.

[15] F. Millo, S. Caputo, C. Cubito, A. Calamiello, D. Mercuri, M. Rimondi, Numerical simulation of the warm-up of a passenger car diesel engine equipped with an advanced cooling system, Tech. rep., SAE Technical Paper (2016).

[16] A. Broatch, P. Olmeda, X. Margot, J. Gómez-Soriano, Numerical simulations for evaluating the impact of advanced insulation coatings on h2 additivated gasoline lean combustion in a turbocharged spark-ignited engine, Applied Thermal Engineering 148 (2019) 674–683. doi:https://doi.org/10.1016/j.applthermaleng.2018.11.106.

[17] F. Berni, S. Fontanesi, A 3d-cfd methodology to investigate boundary layers and assess the applicability of wall functions in actual industrial problems: a focus on in-cylinder simulations, Applied Thermal Engineering (2020) 115320doi:https://doi.org/10.1016/j.applthermaleng.2020.115320.

[18] J. Benajes, R. Novella, J. Gomez-Soriano, I. Barbery, C. Libert, F. Rampanarivo, M. Dabiri, Computational assessment towards understanding the energy conversion and combustion process of lean mixtures in passive pre-chamber ignited engines, Applied Thermal Engineering (2020) 115501doi:https://doi.org/10.1016/j.applthermaleng.2020.115501.

[19] G. Decan, T. Lucchini, G. D'Errico, S. Verhelst, A novel technique for detailed and time-efficient combustion modeling of fumigated dual-fuel internal combustion engines, Applied Thermal Engineering (2020) 115224doi:https://doi.org/10.1016/j.applthermaleng.2020.115224.

[20] P. Olmeda, X. Margot, P. Quintero, J. Escalona, Numerical approach to define a thermodynamically equivalent material for the conjugate heat transfer simulation of very thin coating layers, International Journal of Heat and Mass Transfer 162 (2020) 120377. doi:https://doi.org/10.1016/j.ijheatmasstransfer.2020.120377.

[21] N. Kim, I. Ko, K. Min, Development of a zero-dimensional turbulence model for a spark ignition engine, International Journal of Engine Research 20 (4) (2019) 441–451. doi:https://doi.org/10.1177/1468087418760406.

[22] A. Broatch, X. Margot, R. Novella, J. Gomez-Soriano, Combustion noise analysis of partially premixed combustion concept using gasoline fuel in a 2-stroke engine, Energy 107 (Supplemnet C) (2016) 612–624. doi:https://doi.org/10.1016/j.energy.2016.04.045.

[23] A. Broatch, X. Margot, R. Novella, J. Gomez-Soriano, Impact of the injector design on the combustion noise of gasoline partially premixed combustion in a 2-stroke engine, Applied Thermal Engineering 119 (2017) 530–540. doi:http://dx.doi.org/10.1016/j.applthermaleng.2017.03.081.

[24] S. Cho, C. Song, N. Kim, S. Oh, D. Han, K. Min, Influence of the wall temperatures of the combustion chamber and intake ports on the charge temperature and knock characteristics in a spark-ignited engine, Applied Thermal Engineering 182 (2020) 116000. doi:https://doi.org/10.1016/j.applthermaleng.2020.116000.

[25] M. Garg, R. Ravikrishna, In-cylinder flow and combustion modeling of a cng-fuelled stratified charge engine, Applied Thermal Engineering 149 (2019) 425–438. doi:https://doi.org/10.1016/j.applthermaleng.2018.12.036.

[26] Y. Li, S.-C. Kong, Coupling conjugate heat transfer with in-cylinder combustion modeling for engine simulation, International Journal of Heat and Mass Transfer 54 (11) (2011) 2467 – 2478. doi:https://doi.org/10.1016/j.ijheatmasstransfer.2011.02.015.

[27] E. Urip, K. Liew, S.-L. Yang, Modeling ic engine conjugate heat transfer using the kiva code, Numerical Heat Transfer Part A-applications - NUMER HEAT TRANSFER PT A-APPL 52 (2007) 1–23. doi:10.1080/10407780601112803.

[28] M. Patil, A. Pise, N. Gokhale, Simulation of conjugate heat transfer (cht) between engine head and cooling medium of diesel engine, SAE Technical Papers 2015 (04 2015). doi:10.4271/2015-01-1662.

[29] P. Kundu, R. Scarcelli, S. Som, A. Ickes, Y. Wang, J. Kiedaisch, M. Rajkumar, Modeling heat loss through pistons and effect of thermal boundary coatings in diesel engine simulations using a conjugate heat transfer model, SAE Technical Paper (2016).

[30] M. Wu, Y. Pei, J. Qin, X. Li, J. Zhou, Z. S. Zhan, Q.-y. Guo, B. Liu, T. G. Hu, Study on methods of coupling numerical simulation of conjugate heat transfer and in-cylinder combustion process in gdi engine, WCX™ 17: SAE World Congress Experience (mar 2017). doi:https://doi.org/10.4271/2017-01-0576.

[31] A. Robert, K. Truffin, N. Iafrate, S. Jay, O. Colin, C. Angelberger, Large-eddy simulation analysis of knock in a direct injection spark ignition engine, International Journal of Engine Research 20 (7) (2019) 765–776. doi:https://doi.org/10.1177/1468087418796323.

[32] O. Bolehovskỳ, J. Novotnỳ, Influence of underhood flow on engine cooling using 1-d and 3-d approach, Journal of Middle European Construction and Design of Cars 13 (3) (2015) 24–32.

[33] E. Graziano, L. Bruno, P. Corrado, S. Pierson, G. Virelli, Set-up and validation of an integrated engine thermal model in gt-suite for heat rejection prediction, Tech. rep., SAE Technical Paper (2019).

[34] A. Poubeau, A. Vauvy, F. Duffour, J.-M. Zaccardi, G. d. Paola, M. Abramczuk, Modeling investigation of thermal insulation approaches for low heat rejection diesel engines using a conjugate heat transfer model, International Journal of Engine Research 20 (1) (2019) 92–104. doi:https://doi.org/10.1177/1468087418818264.

[35] A. Broatch, P. Olmeda, X. Margot, J. Escalona, Conjugate heat transfer study of the impact of 'thermo-swing'coatings on internal combustion engines heat losses, International Journal of Engine Research (2020) 1468087420960617doi:https://doi.org/10.1177/1468087420960617.

[36] A. Broatch, P. Olmeda, X. Margot, J. Escalona, New approach to study the heat transfer in internal combustion engines by 3d modelling, International Journal of Thermal Sciences 138 (2019) 405 – 415. doi:https://doi.org/10.1016/j.ijthermalsci.2019.01.006.

[37] A. Broatch, X. Margot, J. Garcia-Tiscar, J. Escalona, Validation and analysis of heat losses prediction using conjugate heat transfer simulation for an internal combustion engine, in: 14th International Conference on Engines Vehicles, SAE International, 2019. doi:https://doi.org/10.4271/2019-24-0091.

[38] Y. Zhang, L. Zhan, Z. He, M. Jia, X. Leng, W. Zhong, Y. Qian, X. Lu, An investigation on gasoline compression ignition (gci) combustion in a heavy-duty diesel engine using gasoline/hydrogenated catalytic biodiesel blends, Applied Thermal Engineering 160 (2019) 113952. `doi:https://doi.org/10.1016/j.applthermaleng.2019.113952`.

[39] Gamma technologies inc., GT-SUITE Theory Manual (2019).

[40] J. Benajes, R. Novella, J. Gǿmez-Soriano, P. J. Martinez-Hernandiz, C. Libert, M. Dabiri, Evaluation of the passive prechamber ignition concept for future high compression ratio turbocharged spark-ignition engines, Applied Energy 248 (12) (2019) 576–588. `doi:https://doi.org/10.1016/j.apenergy.2019.04.131`.

[41] A. J. Torregrosa, P. Olmeda, J. Martín, C. Romero, A tool for predicting the thermal performance of a diesel engine, Heat transfer engineering 32 (10) (2011) 891–904.

[42] F. Carpenter, A. Colburn, Proceedings of general discussion on heat transfer, Inst. Mech. Engrs., London, England (1951) 1–7.

[43] E. Cuthill, Several strategies for reducing the bandwidth of matrices, in: Sparse matrices and their applications, Springer, 1972, pp. 157–166.

[44] J. Chérel, J.-M. Zaccardi, B. Bouteiller, A. Allimant, Experimental assessment of new insulation coatings for lean burn spark-ignited engines, Oil & Gas Science and Technology–Revue d'IFP Energies nouvelles 75 (2020) 11. `doi:https://doi.org/10.2516/ogst/2020006`.

[45] M. G. Masouleh, K. Keskinen, O. Kaario, H. Kahila, S. Karimkashi, V. Vuorinen, Modeling cycle-to-cycle variations in spark ignited combustion engines by scale-resolving simulations for different engine speeds, Applied Energy 250 (2019) 801–820. `doi:https://doi.org/10.1016/j.apenergy.2019.03.198`.

[46] H. M. Cho, B.-Q. He, Spark ignition natural gas engines—a review, Energy conversion and management 48 (2) (2007) 608–618.

[47] D. Jung, K. Sasaki, N. Iida, Effects of increased spark discharge energy and enhanced in-cylinder turbulence level on lean limits and cycle-to-cycle variations of combustion for si engine operation, Applied energy 205 (2017) 1467–1477. `doi:https://doi.org/10.1016/j.apenergy.2017.08.043`.

[48] A. N. Abdalla, O. M. Ali, O. I. Awad, H. Tao, Wavelet analysis of an si engine cycle-to-cycle variations fuelled with the blending of gasoline-fusel oil at a various water content, Energy Conversion and Management 183 (2019) 746–752. `doi:https://doi.org/10.1016/j.enconman.2019.01.034`.

[49] F. Payri, P. Olmeda, J. Martín, A. García, A complete 0d thermodynamic predictive model for direct injection diesel engines, Applied Energy 88 (12) (2011) 4632–4641. `doi:https://doi.org/10.1016/j.apenergy.2011.06.005`.

[50] Y. Lu, X. Zhang, P. Xiang, D. Dong, Analysis of thermal temperature fields and thermal stress under steady temperature field of diesel engine piston, Applied Thermal Engineering 113 (2017) 796 – 812. `doi:https://doi.org/10.1016/j.applthermaleng.2016.11.070`.

[51] J. M. Desantes, J. Benajes, A. García, J. Monsalve-Serrano, The role of the in-cylinder gas temperature and oxygen concentration over low load reactivity controlled compression ignition combustion efficiency, Energy 78 (2014) 854–868. `doi:https://doi.org/10.1016/j.energy.2014.10.080`.